



Cite this: *Chem. Commun.*, 2021,
57, 5806

Received 2nd April 2021,
Accepted 14th April 2021

DOI: 10.1039/d1cc01753e

rsc.li/chemcomm

Transition metal chemistry in synthetically viable alkaline earth complexes $M(\text{Cp})_3^-$ ($M = \text{Ca}, \text{Sr}, \text{Ba}$)[†]

Bin Huo,^{‡a} Rui Sun,^{‡a} Bo Jin,^a Lingfei Hu,^b Jian-Hong Bian,^{id a} Xiao-Ling Guan,^a
Caixia Yuan,^{id a} Gang Lu^b and Yan-Bo Wu^{id *a}

We predicted the stable alkaline earth complexes $M(\text{Cp})_3^-$ ($M = \text{Ca}, \text{Sr}, \text{Ba}$; $\text{Cp} = \text{cyclopentadienyl}$), where the M centers were in their stable +2 oxidation state and mimicked the bonding behaviour of transition metals by participating in bonding with the π orbitals of Cp ligands using their d orbitals.

Having two more electron(s) than noble gases in the previous row of the Periodic Table, alkaline earth (AE) metals tend to lose such outermost valence ns electrons (n is the principal quantum number) to achieve the optimal electronic structures of noble gases. Specifically, the heavy AE (HAE) metals almost always exist in the +2 formal oxidation state,¹ commonly as the positive portions of ionic salts. Nevertheless, the chemistry of HAE metals can be much richer, which is generally related to the bonding involving their d orbitals.² For instance, HAE complexes can be good catalysts,³ as exemplified by a novel nucleophilic alkylation reaction catalysed by calcium, the d orbitals of which participated in the bonding.^{3a} Moreover, such bonding behaviour of HAE metals has been extended to fully mimic transition metals (TMs).⁴ Concrete evidence came from the cubic (O_h) complexes $M(\text{CO})_8$ and $M(\text{N}_2)_8$ ($M = \text{Ca}, \text{Sr}, \text{Ba}$),^{4c,d} which were stabilized by the σ -donation and π -backdonation between the CO or N_2 ligands and the valence $nsnp(n-1)d$ atomic orbitals (AOs) of the HAE centre. Very recently, the TM-like bonding behaviour of HAE metals was further proved by the metallocene-like trisbenzene complexes $M(\text{Bz})_3$ ($M = \text{Ca}, \text{Sr}, \text{Ba}$; $\text{Bz} = \text{benzene}$)^{4e} featuring novel π - d interactions. HAE metals are now regarded as “honorary transition metals”.

Nonetheless, the recently reported complexes, where the HAEs mimicked the TMs, have been realized in trace amounts due to their instabilities, which originate from the zero oxidation state of the HAE (M^0), so they can be generated only under extreme conditions, such as in gas-phase infrared photodissociation spectra or in low-temperature matrix isolation. To our knowledge, none of them has been synthesizable in the condensed phase. In the present work, we report $M(\text{Cp})_3^-$ ($M = \text{Ca}, \text{Sr}, \text{Ba}$, and $\text{Cp} = \text{cyclopentadienyl}$) complexes (see Fig. 1), which are highly viable targets for chemical synthesis in the condensed phase due to their stable components (M^{2+} cations and Cp^- ligands), good molecular stability, and their well-defined electronic structures.

The geometry optimization and subsequent harmonic vibration analysis in this work were performed at the M06-2X-D3^{5,6}/def2-TZVP⁷ level using the Gaussian 16 package.⁸ The relative

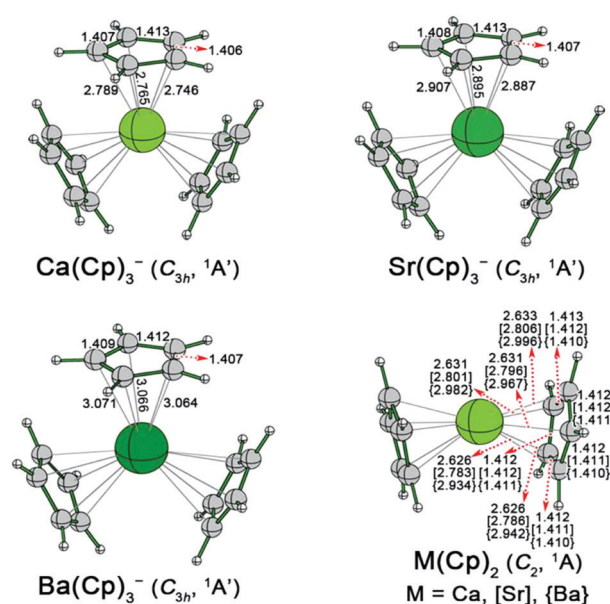


Fig. 1 Optimized structures of $M(\text{Cp})_3^-$ and $M(\text{Cp})_2$ ($M = \text{Ca}, \text{Sr}, \text{Ba}$).

^a Key Laboratory of Materials for Energy Conversion and Storage of Shanxi Province, Institute of Molecular Science, Shanxi University, Taiyuan 030006, People's Republic of China. E-mail: wyb@sxu.edu.cn

^b School of Chemistry and Chemical Engineering, Shandong University, Jinan, 250100, People's Republic of China

[†] Electronic supplementary information (ESI) available: The MO correlation diagram of $M(\text{Cp})_3^-$ ($M = \text{Sr}$ and Ba), the optimized structures of $\text{Na}[M(\text{Cp})_3]$ ($M = \text{Ca}, \text{Sr}, \text{Ba}$), the results concerning the effects of Me-substitution for Cp ligands, and the Cartesian coordinates of optimized structures of the species reported in the text. See DOI: 10.1039/d1cc01753e

[‡] Bin Huo and Rui Sun contributed equally to this work.

energies were compared at the CCSD(T)⁹/M06-2X level, where CCSD(T)/M06-2X denotes the single point energies at the CCSD(T)/def2-TZVPP level plus the Gibbs free energy corrections at the M06-2X-D3/def2-TZVPP level and 298 K.

Our work was initiated from the attempt to further stabilize $M(\text{Bz})_3$ ($M = \text{Ca}, \text{Sr}, \text{Ba}$) complexes.^{4e} As shown in Table 1, the instability of the previously reported neutral $M(\text{Bz})_3$ complexes can be reflected by the high energy levels of their HOMOs (−3.00 to −3.24 eV) and the low total binding energies (BEs) of −8.7 to −19.5 kcal mol^{−1}. The problems may be attributed to the M^0 state of the HAE metals. Therefore, we propose to employ the M^{2+} cation for designing the $M(\text{Bz})_3$ -like species. Herein, we were inspired by the chemical similarity between Ca^{2+} and Ln^{3+} (Ln denotes Sc, Y, or the lanthanide metals) and the structures of synthesized $\text{Ln}(\text{Cp})_3$ complexes,¹⁰ which are similar in molecular shape to the $M(\text{Bz})_3$ complexes. Substituting the Ln atom in $\text{Ln}(\text{Cp})_3$ with Ca or its heavy congeners Sr or Ba and simultaneously adding a negative charge to maintain the skeletal electrons, we could obtain the anionic $M(\text{Cp})_3^-$ complexes ($M = \text{Ca}, \text{Sr}, \text{Ba}$). As shown in Fig. 1, they are all the energy minima adopting C_{3h} symmetry with three Cp^- ligands arranged in head-to-tail manner around the central HAE. The C–C bond lengths in the $M(\text{Cp})_3^-$ complexes range from 1.407 to 1.413 Å, very close to that of 1.408 Å found in the free Cp^- ligand. Since no C–C bond lengths in the Cp^- ligands are obviously elongated upon the formation of the $M(\text{Cp})_3^-$ complexes, it seems that there is no electron backdonation from the valence AO of the HAE to the antibonding orbital(s) of the Cp ligands, *i.e.* the HAEs in the $M(\text{Cp})_3^-$ complexes may be in their +2 formal oxidation state.

To verify this deduction, molecular orbital (MO) correlation analyses were performed. As exemplified by the diagram of $\text{Ca}(\text{Cp})_3^-$ shown in Fig. 2, there are nine doubly occupied MOs concerning the valence 4s4p3d AOs of the Ca atoms and the π orbitals of the Cp ligands, so it obeys the 18-electron rule. As Fig. 2 shows, the HOMO–13, degenerate HOMO–8, and HOMO–2 of $\text{Ca}(\text{Cp})_3^-$ originate from the $\text{Cp} \rightarrow \text{Ca}$ donation concerning the s, p_x/p_y , and p_z AOs, respectively, the degenerate HOMO–3 and degenerate HOMO–1 stem from the $\text{Cp} \rightarrow \text{Ca}$ donation of concerning the $d_{xy}/d_{x^2-y^2}$ and d_{xz}/d_{yz} AOs,

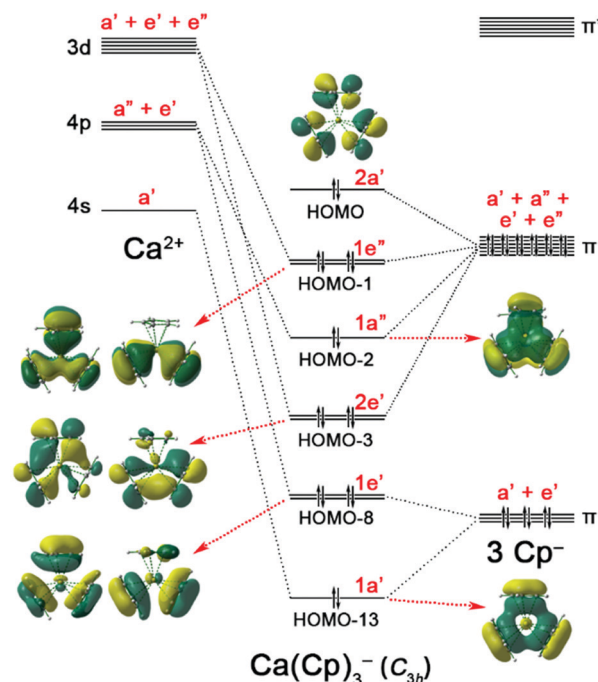


Fig. 2 MO correlation diagram of Ca^{2+} with three Cp^- ligands.

respectively, while the HOMO is a ligand-only orbital. It is obvious that the $\text{Ca}(\text{Cp})_3^-$ complex possesses ligand-to-metal donation but does not possess metal-to-ligand backdonation, so the Ca atom should be in its +2 oxidation state. The diagrams of the $\text{Sr}(\text{Cp})_3^-$ and $\text{Ba}(\text{Cp})_3^-$ complexes are similar to that of the $\text{Ca}(\text{Cp})_3^-$ complex and they are given in Fig. S1 and S2 in the ESI.[†]

The $M(\text{Cp})_3^-$ complexes ($M = \text{Ca}, \text{Sr}, \text{Ba}$) are stabilized substantially by the favourable Coulombic interactions between the positively charged M^{2+} centre and the negatively charged Cp^- ligands. As shown in Table 1, the binding energies (BEs) relative to M^{2+} and three Cp^- ligands are −514.4, −500.5, and −474.3 kcal mol^{−1} for $M = \text{Ca}, \text{Sr}, \text{Ba}$, respectively. As suggested by our reviewer, we computed the reduction potentials based on such binding energies (see ESI[†] for details), generating the results of −13.99, −13.72, and −13.16 V for $M = \text{Ca}, \text{Sr}$, and Ba , respectively, which indicated that the M^{2+} ions in these complexes were extremely difficult to be reduced. As a comparison, the interactions between $M(\text{Cp})_2$ (see Fig. 1) and Cp^- do not involve the neutralization of negative and positive charges, and the corresponding BEs are as low as −40.1 to −49.9 kcal mol^{−1}. Nevertheless, these values are still significantly higher than the total BEs of $M(\text{Bz})_3$ (−6.5 to −14.2 kcal mol^{−1}), which suggest the rather high affinity irrelevant to the direct electrostatic interactions. Note that two Cp ligands in the $M(\text{Cp})_2$ complexes (Fig. 1) are not arranged face-to-face, but in an edge-to-edge manner, leaving an open site, which is ready for binding the third Cp^- ligand. The total binding energies among an M atom, two neutral Cp ligands, and an anionic Cp^- ligand to give $M(\text{Cp})_3^-$ were calculated to be −177.2 to −199.9 kcal mol^{−1}, also revealing the high affinity between the M centre and the Cp ligands.

Table 1 The lowest vibrational frequencies (ν_{min}) in cm^{−1}, the HOMO energy levels (E_{HOMO}), the HOMO–LUMO gaps (gap), the VDEs, and VEA in eV, and the total binding energies (BE_{Tot} in kcal mol^{−1}) with regard to free positive and negative ions, and that for binding the third Cp^- (BE_{Cp} in kcal mol^{−1}) at the CCSD(T)/M06-2X-D3 level

	ν_{min}	E_{HOMO}	Gap	VDE	VEA	BE_{Tot}	BE_{Cp}
$\text{D}_3 \text{Ca}(\text{Bz})_3$	39	−3.24	3.12	3.72	1.44	−8.7 ^a	−6.5 ^a
$\text{D}_3 \text{Sr}(\text{Bz})_3$	25	−3.10	2.91	3.57	1.12	−11.0 ^a	−14.2 ^a
$\text{D}_3 \text{Ba}(\text{Bz})_3$	21	−3.00	2.75	3.39	0.74	−19.5 ^a	−13.4 ^a
$\text{C}_{3h} \text{Ca}(\text{Cp})_3^-$	44	−2.69	5.90	3.32	4.18	−40.1	−514.4
$\text{C}_{3h} \text{Sr}(\text{Cp})_3^-$	31	−2.93	5.87	3.57	3.91	−47.6	−500.5
$\text{C}_{3h} \text{Ba}(\text{Cp})_3^-$	24	−3.15	5.56	3.81	3.15	−49.9	−474.3
$\text{C}_3 \text{Na}[\text{Ca}(\text{Cp})_3]$	31	−6.18	4.75	6.78	−0.45	−120.8	−608.3
$\text{C}_3 \text{Na}[\text{Sr}(\text{Cp})_3]$	27	−6.32	4.98	6.93	−0.37	−124.9	−592.8
$\text{C}_3 \text{Na}[\text{Ba}(\text{Cp})_3]$	5	−6.42	5.20	7.03	−0.24	−126.2	−568.9

^a The results were reported at the M06-2X-D3/def2-TZVPP level.

Table 2 ALMO-EDA results for $M(\text{Cp})_3^-$ complexes ($M = \text{Ca}, \text{Sr}, \text{Ba}$). The total interaction energies (ΔE_{int}) between the fragments were divided into repulsive interactions (Pauli repulsion, ΔE_{Pauli}) and attractive interactions (ΔE_{attr}), including electrostatics (ΔE_{elstat}), dispersion (ΔE_{disp}), polarization (ΔE_{pola}), and charge transfer (ΔE_{ct})

M	$[\text{M}^{2+} + 3\text{Cp}^-]$			$[\text{M}(\text{Cp})_2 + \text{Cp}^-]$		
	Ca	Sr	Ba	Ca	Sr	Ba
ΔE_{int}	−766.0	−729.3	−692.6	−68.4	−68.6	−66.2
ΔE_{Pauli}	77.9	91.2	113.2	53.6	46.3	48.8
ΔE_{attr}	−843.9	−820.4	−805.9	−122.0	−114.9	−115.0
ΔE_{elstat}	−658.8	−646.6	−628.7	−68.3	−66.0	−63.7
ΔE_{disp}	−15.1	−18.9	−23.9	−20.3	−17.5	−15.6
ΔE_{pola}	−141.8	−125.0	−114.2	−23.1	−20.2	−19.8
ΔE_{ct}	−28.3	−29.9	−39.0	−10.3	−11.3	−15.9

To get more details on the metal–ligand bonding, ALMO-EDA¹¹ analysis was performed at the M06-2X-D3/def2-TZVPP level using the Q-Chem Package.¹² Two schemes for fragment partition were studied, including $[\text{M}^{2+} + 3\text{Cp}^-]$ (scheme I) and $[\text{M}(\text{Cp})_2 + \text{Cp}^-]$ (scheme II). As shown in Table 2, the values of the total interaction energies (ΔE_{int}) for scheme I are very high (−692.6 to −766.0 kcal mol^{−1}). Of the various interaction energies, the electrostatics (ΔE_{elstat}) played the most important role, as reflected by the highly negative values of −628.7 to −658.8 kcal mol^{−1}, accounting for 78.0% to 78.8% of the total attractive interactions (ΔE_{attr}). The favourable Coulombic interactions greatly stabilize the complexes. Though the polarization and charge transfer energies (ΔE_{pola} and ΔE_{ct}) were relatively low in comparison with ΔE_{elstat} , their absolute values are high, being −114.2 to −141.8 kcal mol^{−1} for ΔE_{pola} and −28.3 to −39.0 kcal mol^{−1} for ΔE_{ct} , suggesting the important role played by the valence AOs of the metal centers because ΔE_{pola} and ΔE_{ct} may concern the d-orbital bonding and the coordination to metal, respectively. Given that M atoms are regarded as dications (+2 |e|) in $\text{M}(\text{Cp})_3^-$ complexes, the CM5 charges¹³ of +0.64 to +0.75 indicate the obvious charge transfer to the M centres.

The ΔE_{int} values for the scheme II are −66.2 to −68.4 kcal mol^{−1}, significantly lower than those for the scheme I. This is understandable because scheme II does not involve the neutralization of positive and negative ions. Nevertheless, the ΔE_{elstat} values of −63.7 to −68.3 kcal mol^{−1} still account for 55.4%–57.4% of the ΔE_{attr} values. Like the situation for the scheme I, the ΔE_{pola} (−19.8 to −23.1 kcal mol^{−1}) and ΔE_{ct} (−10.3 to −15.9 kcal mol^{−1}) also played the important roles though they are significantly smaller than the ΔE_{elstat} . Nonetheless, the dispersion energies (ΔE_{disp} , −15.6 to −20.3 kcal mol^{−1} with ΔE_{int} value of −66.2 to −68.4 kcal mol^{−1}) in scheme II played a more significant role than that in the scheme I (−15.1 to −23.9 kcal mol^{−1} with ΔE_{int} value of −692.6 to −766.0 kcal mol^{−1}).

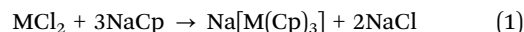
The designed complexes were found to possess a well-defined electronic structure. First, the nine orbitals shown in Fig. 2 are all doubly occupied, leading to the singlet ¹A' ground electronic state. Second, as the negative ions, their low HOMO energy levels of −2.69 to −3.15 eV are similar to those of the neutral $\text{M}(\text{Bz})_3$ complexes, while the energy levels of the lowest unoccupied MOs (LUMOs) are much higher than those of $\text{M}(\text{Bz})_3$, leading to HOMO–LUMO gaps of 5.56–5.90 eV, which

are much wider than those of the $\text{M}(\text{Bz})_3$ complexes (at 2.75–3.12 eV). Third, as shown in Table 1, the $\text{M}(\text{Cp})_3^-$ complexes were also stable regarding the electron gain and loss, as revealed by the high vertical detachment energies (VDEs) of 3.32–3.81 eV and positive vertical electron affinities (VEAs) of 3.15–4.18 eV. The VDEs are akin to that of Cl^- (3.62 eV, the highest VDEs for atomic anions in the Periodic Table), indicating the low tendency to lose an electron, while their positive VEAs suggest that they tend not to obtain an electron.

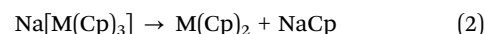
We further studied their kinetic stability by 100 picosecond Born–Oppenheimer molecular dynamic (BOMD) simulations at 298 and 500 K.¹⁴ The root-mean-square derivation (RMSD, in Å, relative to the optimized structures) was employed to describe the structural evolution. As shown in Fig. S3 (ESI[†]), all RMSD plots do not have the meaningful upward jump, suggesting that the structures of the $\text{M}(\text{Cp})_3^-$ ($M = \text{Ca}, \text{Sr}, \text{Ba}$) complexes are rather rigid. Simultaneously, the fluctuation of RMSD values is small, as mirrored by the average RMSD values of 0.08 and 0.11 Å as well as the variation ranges of 0.02–0.23 Å and 0.02–0.37 Å for the simulations at 298 and 500 K, respectively. Therefore, the $\text{M}(\text{Cp})_3^-$ complexes are kinetically stable against isomerization or dissociation.

We were recently informed that the crystalline structures with the formula of $[\text{Ca}(\text{Cp}_3)\text{THF}]^-$ and $\text{Ba}(\text{Cp}_3)^-$ complexes had been reported previously.¹⁵ Nevertheless, the crystalline structures of the $\text{Ca}(\text{Cp}_3)^-$ and $\text{Ba}(\text{Cp}_3)^-$ complexes are different from those shown in Fig. 1 in that the former had an additional tetrahydrofuran (THF) ligand and the latter adopted a polymeric arrangement, where each Ba atom was surrounded by four Cp ligands. Nonetheless, the existence of such similar structures revealed the possible realization of our structures in the experiments.

Looking at the synthetic route of the $\text{Ln}(\text{Cp})_3$ complexes, we propose here a metathesis reaction (see eqn (1)) with sodium cyclopentadienide (NaCp) and HAE chlorides (MCl_2) as the reactants to generate the sodium salt of $\text{M}(\text{Cp})_3^-$, *i.e.* $\text{Na}[\text{M}(\text{Cp})_3]$ ($M = \text{Ca}, \text{Sr}, \text{Ba}$), and sodium chloride (NaCl). Eqn (1) is exergonic by −20.1, −24.9, and −29.1 kcal mol^{−1} for $M = \text{Ca}, \text{Sr}$, and Ba , respectively, at the CCSD(T)//M06-2X level, suggesting that the designed metathesis reaction for the generation of $\text{M}(\text{Cp})_3^-$ is thermodynamically favourable.



The neutralization of anionic $\text{M}(\text{Cp})_3^-$ complexes by the Na^+ cation is highly exergonic, being −93.9, −92.3, and −94.6 kcal mol^{−1} for $M = \text{Ca}, \text{Sr}, \text{Ba}$, respectively, at the CCSD(T)//M06-2X level. We further studied the dissociation of $\text{Na}[\text{M}(\text{Cp})_3]$ into two neutral fragments of $\text{M}(\text{Cp})_2$ and NaCp (see eqn (2)):



The dissociation energies were 0.1, 5.9, and 10.6 kcal mol^{−1} for $M = \text{Ca}, \text{Sr}$, and Ba , respectively, at the CCSD(T)//M06-2X level, suggesting that dissociation of the $\text{Na}[\text{M}(\text{Cp})_3]$ complexes is endergonic. As shown in Fig. S4 (ESI[†]), the neutralized salt complexes $\text{Na}[\text{M}(\text{Cp})_3]$ ($M = \text{Ca}, \text{Sr}, \text{Ba}$) all adopt the C_3 geometry with the Na atom located at the three-fold axis of

the $\text{M}(\text{Cp})_3$ moiety. In comparison with the anionic $\text{M}(\text{Cp})_3^-$ complexes, the neutralized $\text{Na}[\text{M}(\text{Cp})_3]$ complexes possess significantly lowered HOMO energy levels (-6.18 to -6.42 eV versus -2.69 to -3.15 eV) and slightly narrowed HOMO–LUMO gaps (4.75 – 5.20 eV versus 5.56 – 5.90 eV). It can be expected that the $\text{M}(\text{Cp})_3^-$ complexes may be realized as the negative portion of an ionic salt.

In summary, we have demonstrated, based on extensive computational studies, that the heavy alkaline earth (HAE) metals in $\text{M}(\text{Cp})_3^-$ ($\text{M} = \text{Ca}, \text{Sr}, \text{Ba}$) complexes exhibit the bonding behaviour that is typical of transition metals (TMs) by participating in the bonding with d orbitals and fulfilling the 18-electron rule. Different from the previously reported similar category of complexes, which can be generated only in trace amounts due to the instability originating from the M^0 oxidation state of the HAE metals, the $\text{M}(\text{Cp})_3^-$ complexes possess the HAE elements in the +2 oxidation state, leading to good thermodynamic and kinetic stabilities as well as well-defined electronic structures, beneficial for their synthesis. The feasibility of synthesizing these complexes was further indicated by the proposed exergonic metathesis reaction and the high binding energies either between M^{2+} and Cp^- or between M^0 and Cp/Cp^- . The results from this work provide the new evidence for the heavy alkaline earth metals to be considered as honorary transition metals.

This work was supported financially by NSFC (Grant No. 22073058, 21973055 and 21720102006), the Natural Science Foundation of Shanxi Province (Grant No. 201901D111018 and 201901D111014), the OIT Program, the Shanxi “1331 Project” Engineering Research Center (PT201807), the Shanxi 1331KIRT, the Central Government’s Special Fund for Local Science and Technology Development (YDZX20191400002916) and the HPC of Shanxi University.

Note added in proof

After initial publication, it was noted that $[\text{Cp}_3\text{Ca}]^-$ and $[\text{Cp}_3\text{Ba}]^-$ complexes related to those reported in this article have been published in the literature. Therefore, this article has been amended to include discussion of additional references 13, 15a and 15b.

Conflicts of interest

There are no conflicts to declare.

References

- 1 N. N. Greenwood and A. Earnshaw, *Chemistry of the Elements*, Butterworth-Heinemann, Oxford, 2nd edn, 1997, pp. 107–138.
- 2 (a) K. M. Fromm, *Coord. Chem. Rev.*, 2020, **408**, 213193; (b) I. Fernández, N. Holzmann and G. Frenking, *Chem. – Eur. J.*, 2020, **26**, 14194–14210.
- 3 (a) A. S. S. Wilson, M. S. Hill, M. F. Mahon, C. Dinioi and L. Maron, *Science*, 2017, **358**, 1168; (b) H. Bauer, M. Alonso, C. Färber, H. Elsen, J. Pahl, A. Cauzero, G. Ballmann, F. De Proft and S. Harder, *Nat. Catal.*, 2018, **1**, 40–47; (c) H. Bauer, M. Alonso, C. Fischer, B. Rösch, H. Elsen and S. Harder, *Angew. Chem., Int. Ed.*, 2018, **57**, 15177–15182; (d) P. B. Armentrout, *Science*, 2018, **361**, 849; (e) X. Yang, *Natl. Sci. Rev.*, 2018, **6**, 8–9; (f) P. J. Chirik, *Organometallics*, 2019, **38**, 195–197; (g) T. Bettens, S. Pan, F. De Proft, G. Frenking and P. Geerlings, *Chem. – Eur. J.*, 2020, **26**, 12785–12793.
- 4 (a) M. Kaupp, *Angew. Chem., Int. Ed.*, 2001, **40**, 3534–3565; (b) L. Gagliardi and P. Pykkö, *Theor. Chem. Acc.*, 2003, **110**, 205–210; (c) X. Wu, L. Zhao, J. Jin, S. Pan, W. Li, X. Jin, G. Wang, M. Zhou and G. Frenking, *Science*, 2018, **361**, 912–916; (d) Q. Wang, S. Pan, S. Lei, J. Jin, G. Deng, G. Wang, L. Zhao, M. Zhou and G. Frenking, *Nat. Commun.*, 2019, **10**, 3375; (e) Q. Wang, S. Pan, Y.-B. Wu, G. Deng, J.-H. Bian, G. Wang, L. Zhao, M. Zhou and G. Frenking, *Angew. Chem., Int. Ed.*, 2019, **58**, 17365–17374; (f) H.-R. Li, X.-Q. Lu, Y.-Y. Ma, Y.-W. Mu, H.-G. Lu, Y.-B. Wu and S.-D. Li, *J. Cluster Sci.*, 2019, **30**, 621–626; (g) X. Wu, L. Zhao, D. Jiang, I. Fernández, R. Berger, M. Zhou and G. Frenking, *Angew. Chem., Int. Ed.*, 2018, **57**, 3974–3980.
- 5 Y. Zhao and D. G. Truhlar, *Theor. Chem. Acc.*, 2008, **120**, 215–241.
- 6 S. Grimme, J. Antony, S. Ehrlich and H. Krieg, *J. Chem. Phys.*, 2010, **132**, 154104.
- 7 (a) F. Weigend and R. Ahlrichs, *Phys. Chem. Chem. Phys.*, 2005, **7**, 3297–3305; (b) F. Weigend, *Phys. Chem. Chem. Phys.*, 2006, **8**, 1057–1065.
- 8 M. J. Frisch, G. W. Trucks and H. B. Schlegel, *et al.*, *Gaussian 16 (Revision A.03)*, Gaussian, Inc., Wallingford, CT, 2016.
- 9 K. Raghavachari, G. W. Trucks, J. A. Pople and M. Head-Gordon, *Chem. Phys. Lett.*, 1989, **157**, 479–483; the frozen core was NOT used in the CCSD(T) calculations and the T1-diagnostic values were less than 0.011, which excluded the necessity to consider the multi-reference characters.
- 10 See for example (a) G. Wilkinson and J. M. Birmingham, *J. Am. Chem. Soc.*, 1954, **76**, 6210; (b) J. M. Birmingham and G. Wilkinson, *J. Am. Chem. Soc.*, 1956, **78**, 42–44; (c) E. O. Fischer and H. Fischer, *J. Organomet. Chem.*, 1965, **3**, 181–187; (d) W. Hinrichs, D. Melzer, M. Rehwoldt, W. Jahn and R. D. Fischer, *J. Organomet. Chem.*, 1983, **251**, 299–305.
- 11 P. R. Horn, Y. Mao and M. Head-Gordon, *Phys. Chem. Chem. Phys.*, 2016, **18**, 23067–23079.
- 12 Y. Shao, Z. Gan and E. Epifanovsky, *et al.*, *Mol. Phys.*, 2015, **113**, 184–215.
- 13 A. V. Marenich, S. V. Jerome, C. J. Cramer and D. G. Truhlar, *J. Chem. Theory Comput.*, 2012, **8**, 527–541.
- 14 (a) The BOMD simulations were performed at the PBE^{14b}/DZVP^{14c} level using CP2K package^{14d}; (b) J. P. Perdew, K. Burke and M. Ernzerhof, *Phys. Rev. Lett.*, 1996, **77**, 3865–3868; (c) J. VandeVondele and J. Hutter, *J. Chem. Phys.*, 2007, **127**, 114105; (d) T. D. Kühne and J. Hutter, *J. Chem. Phys.*, 2020, **152**, 194103.
- 15 (a) S. Harder, *Angew. Chem., Int. Ed.*, 1998, **37**, 1239–1241; (b) R. Fischer, J. Langer, S. Kriek, H. Görls and M. Westerhausen, *Organometallics*, 2011, **30**, 1359–1365.